Short-term high fat diet alters genes associated with metabolic and vascular dysfunction during adolescence in rats: a pilot study

Alex E. Mohr[1], Rebecca A. Reiss[2], Monique Beaudet[2], Johnny Sena[3], Jay S. Naik[4], Benjimen R. Walker[4] and Karen L. Sweazea[5]

[1] College of Health Solutions, Arizona State University, Phoenix, AZ, United States
[2] Biology Department, New Mexico Institute of Mining and Technology, Socorro, NM, United States
[3] National Center for Genome Resources, Santa Fe, NM, USA
[4] The Department of Cell Biology and Physiology, University of New Mexico, Albuquerque, NM, United States
[5] College of Health Solutions & School of Life Sciences, Arizona State University, Tempe, AZ, USA

Corresponding author
Karen L. Sweazea,
Karen.Sweazea@asu.edu

ABSTRACT

Background: Diet-induced metabolic dysfunction precedes multiple disease states including diabetes, heart disease, and vascular dysfunction. The critical role of the vasculature in disease progression is established, yet the details of how gene expression changes in early cardiovascular disease remain an enigma. The objective of the current pilot project was to evaluate whether a quantitative assessment of gene expression within the aorta of six-week old healthy male Sprague-Dawley rats compared to those exhibiting symptoms of metabolic dysfunction could reveal potential mediators of vascular dysfunction.

Methods: RNA was extracted from the aorta of eight rats from a larger experiment; four animals fed a high-fat diet (HFD) known to induce symptoms of metabolic dysfunction (hypertension, increased adiposity, fasting hyperglycemia) and four age-matched healthy animals fed a standard chow diet (CHOW). The bioinformatic workflow included Gene Ontology (GO) biological process enrichment and network analyses.

Results: The resulting network contained genes relevant to physiological processes including fat and protein metabolism, oxygen transport, hormone regulation, vascular regulation, thermoregulation, and circadian rhythm. The majority of differentially regulated genes were downregulated, including several associated with circadian clock function. In contrast, leptin and 3-hydroxy-3-methylglutaryl-CoA synthase 2 (Hmgcs2) were notably upregulated. Leptin is involved in several major energy balance signaling pathways and Hmgcs2 is a mitochondrial enzyme that catalyzes the first reaction of ketogenesis.

Conclusion: Together, these data describe changes in gene expression within the aortic wall of HFD rats with early metabolic dysfunction and highlight potential pathways and signaling intermediates that may impact the development of early vascular dysfunction.

INTRODUCTION

The prevalence of metabolic syndrome has increased among US adults by over 35% since 2012 and currently over two-thirds of Americans meet the diagnostic criteria (*Moore, Chaudhary & Akinyemiju, 2017*). Metabolic syndrome is a cluster of biological factors characterized by abdominal obesity, dyslipidemia, hypertension, and fasting hyperglycemia (*Kassi et al., 2011*). These factors promote cardiometabolic dysfunctions including hypertension, atherosclerosis, aging, heart and renal failure, as well as coronary syndrome (*Cuspidi et al., 2018*; *Katsiki et al., 2014*). Many of these dysfunctions are related to the vasculature and are critical accelerants of cardiovascular disease (CVD), the leading cause of death in the United States (*Benjamin et al., 2019*). The treatment of progressive vascular degeneration is largely hindered by vascular remodeling, which occurs during the progression from a healthy state to a diseased state (*Petrie, Guzik & Touyz, 2018*). In addition, lack of data on the impact of poor diet during adolescence on health as an adult and risk for CVD further complicates efforts to better delineate vascular disease progression and identification of prevention strategies (*Dahm et al., 2016*; *Ning et al., 2015*).

The pathology of vascular dysfunction is multifaceted and can be characterized as a pro-contractile, pro-inflammatory, and pro-coagulant environment at the level of the vascular wall. Molecular components of vascular dysfunction include an imbalance between endothelial-derived vasodilator and vasoconstrictor factors, increased expression of cellular adhesion molecules and pro-inflammatory cytokines, and increased expression of pro-coagulant factors (*Gimbrone & García-Cardeña, 2016*). Vascular dysfunction research has largely focused on protein-level signaling pathways and molecular processes. Associated gene expression changes provide invaluable insight into the genomic-level mechanisms that underlie CVD and facilitate early detection and the development of potential reversal methods for CVD.

When compared to microarray technology, RNA-Seq eliminates the need for *a priori* information necessary for designing primers, provides a less biased view of gene expression, and allows the whole transcriptome to be assayed (*Rao et al., 2019*). The development of post-sequencing bioinformatic workflows to effectively analyze and visualize the data is still in progress, including issues regarding the number of biological replicates and the statistical methods used for small sample sizes (*Li et al., 2020*). The expense of RNA-seq often requires compromising the number of replicates. RNA-seq is highly reproducible, so technical replicates, in which the same nucleic sample is subjected to sequencing multiple times, are unnecessary (*Marioni et al., 2008*). Statistical algorithms used for RNA-seq are designed to compensate for a low number of biological replicates and can detect differential gene expression even when no replicates are available (*Maza, 2016*). There are multiple software packages to accomplish the mapping and statistical analyses and it may be necessary to use different methods on a dataset to select the optimal workflow, which can include the comparison of multiple statistical

methods on the same data (*Kvam, Liu & Si, 2012*). Additional downstream statistics, such as those used to create networks, provide biological significance to the data set. For example, statistical significance can be augmented with biological significance evaluation in the form of Gene Ontology (GO) terms enrichment tests (*Chagoyen & Pazos, 2010*). Biological Process (BP) terms are relevant to this study. However, a list of GO BP terms over-represented by the differentially regulated genes can be difficult to fully interpret. Network analysis can help detect the relationships between the biological processes and changes in gene expression relevant to the experiment. For example, using a workflow with two conditions, each with two replicates that consisted of pooled cells exposed to titanium of a specific grain size, gene expression differences revealed changes in biological processes associated with mechanotransduction (*Reiss et al., 2020*). Cytoscape and associated applications combine data-mining applications with network analysis that facilitate the visualization of data, resulting in an improved understanding of data (*Bindea et al., 2009*; *Cline et al., 2007*). Thus, examination of gene expression response in the vasculature during metabolic dysfunction provides a unique perspective on its pathophysiology and a means to identify potential molecular targets that are missed by conventional methods.

Current understanding of the early changes in gene expression leading to vascular dysfunction, especially during adolescence, remain limited. In addition, there is a paucity of studies that have examined the effects of short-term intake of a high fat diet (HFD) on gene expression within the aorta (*Bao et al., 2016*; *Xi et al., 2017*). RNA-Seq can provide important insights into gene expression and associated molecular mechanisms occurring in early stage vascular dysfunction. Therefore, the objective of the current pilot project was to demonstrate that a quantitative assessment of gene expression within the vascular wall (thoracic aorta) of healthy adolescent male rats compared to those exhibiting metabolic dysfunction could reveal potential pathways and signaling intermediates that contribute to vascular dysfunction. Specifically, we sought to identify genes differentially expressed between HFD and standard Chow-fed rats. When maintained on a HFD, these animals exhibit symptoms of metabolic dysfunction including hypertension, weight gain, glucose intolerance, and insulin insensitivity, which closely resembles the human condition (*Hintze et al., 2018*). Samples analyzed in the present study were obtained from rats that were part of a larger experiment (*Sweazea, Lekic & Walker, 2010*). Briefly, rats on the HFD had significantly greater total body mass, epididymal fat pad mass, waist circumference, fasting whole blood glucose, and systolic blood pressure in addition to impaired endothelium-dependent vasodilation and hyperleptinemia. The HFD rats exhibited symptoms of metabolic syndrome but were not yet diabetic or overtly obese. Therefore, we hypothesized that rats fed HFD would display altered expression of genes associated with vascular dysfunction and metabolic disease. To test this hypothesis, RNA isolated from the aorta of rats that were fed either a HFD or standard Chow diet (CHOW) for six weeks were sequenced and compared to detect changes in gene expression.

MATERIALS & METHODS

Animal experimental protocol

The male Sprague-Dawley rats (140–160 g, 5–6 weeks of age) used in this study were part of a larger investigation that compared symptoms of metabolic dysfunction in rats on CHOW and HFD treatments (*Sweazea, Lekic & Walker, 2010*). The composition of each diet has been described previously (*Crawford et al., 2019*). Briefly, the CHOW diet is the regular maintenance diet of the animals and contained in calories: 18.9% protein, 57.33% carbohydrates (% sucrose NA), and 5% fat (Cat. No. 2018; Harlan Teklad). Half of the animals were switched to a HFD after arrival that modeled a Western diet high in animal-based ingredients and saturated fat. The macronutrient profile of the HFD was 20% protein, 20% carbohydrates (6.8% sucrose) and 60% fat (in %kcal), primarily from lard (Cat. No. D12492; Research Diets, Inc., New Brunswick, NJ, USA) as described by *Crawford et al. (2019)*. This HFD was intentionally selected to be greater than 50% fat to induce and study more severe metabolic syndrome (*Rodríguez-Correa et al., 2020*). In contrast, the fat content of the chow diet was plant-derived (60% soybean oil and meal, 40% wheat and corn). Similarly, the protein composition of the HFD included a mixture of casein, lactic, and 30 mesh whereas the chow diet was comprised of 36% wheat, 34% corn and 26% soy proteins. The carbohydrate composition of the chow diet included 54% wheat products, 40% corn products, and 6% soybean meal whereas the high fat diet included 63% corn and 37% sucrose.

Rats were maintained on the respective diets for 6 weeks and the food was replaced every 2–3 days to prevent spoiling. All animals had access to food and water *ad libitum* and were pair-housed in identical cages in the same animal facility and exposed to a 12:12 h light dark cycle. Animal care procedures were reviewed and approved by the Institutional Animal Care and Use Committee of the University of New Mexico School of Medicine (AAALAC # 000222). The thoracic aorta (not including the aortic arch) of eight animals, four each from the normal CHOW and HFD, were removed, cleared of surrounding fat and connective tissue, and the lumen was cleared of blood. The aortic tissue was placed in RNA later (Qiagen, Valencia, CA, USA) and frozen (−80 °C). Total RNA was extracted with the Qiagen RNeasy kit. RNA from two rats was pooled for each library (CHOW1, CHOW2, HFD1, HFD2), so four animals are represented for each treatment and were contained within two libraries. The high reliability of Illumina sequencing eliminates the need for technical replicates (*Marioni et al., 2008*) so each library was sequenced once.

Library preparation and sequencing

Illumina cDNA libraries were constructed and sequenced at the National Center for Genome Resources (NCGR, Santa Fe, NW) using manufacturer's standard operating protocols. One μg of total RNA for each sample was subjected to Illumina mRNA-SeqPrep Kit RS-100-0801 following manufacturer's protocols. This involved two rounds of polyA selection using polyT beads, random fragmentation of RNA, random priming to make cDNA, ligation of bar-coded sequencing primers, and size selection. The bar-coded

libraries were run in a single lane of a flow cell on an Illumina Genome Analyzer IIx, resulting in single-end 36 nucleotide (nt) read lengths. Raw data files (.fastq) and processed data files are available through the Gene Expression Omnibus (GEO), accession number GSE147335.

The post-sequencing bioinformatic workflow is diagramed in Fig. 1. Four raw data files, two each for the CHOW and HFD condition were uploaded into Lumenogix. Data quality parameters included FASTQC (*Andrews, 2010*, http://www.bioinformatics.babraham.ac. uk/projects/fastqc/) and BLAST (*Altschul et al., 1990*) analysis of randomly selected reads. Reads were mapped to ENSEMBL release 79 of the rat genome (Rnor_5.0; GCA_000001895.3) using two methods, the Genomic Mapping and Alignment Program (GMAP) (*Wu & Watanabe, 2005*) and Tophat, which takes into account potential RNA splice sites, known as splice-site junction mapping (SJM) (*Trapnell, Pachter & Salzberg, 2009*). The results for each mapping program was quantitated per gene using HTSeq count (*Anders, Pyl & Huber, 2015*). The resulting files were archived in GEO (accession number GSE147335). Empirical Analysis of Digital Gene Expression data in R (EdgeR) (*Robinson, McCarthy & Smyth, 2010*) was used to evaluate statistical significance for the GMAP and SJM mapping methods, these results are also archived under GEO GSE147335.
The resulting data files were downloaded and opened with JMP version 14 (SAS Institute, Cary, NC, USA) for data filtering and further analyses. Zipf's power law is a graphic method employed to model complex phenomena (*Adamic, 2011*) that has been used to identify low count theshold in environmental metagenomic shotgun sequence data (*Reiss, Guerra & Makhnin, 2016*) and in a study of cell response to nanostructured titanium (*Reiss et al., 2020*). Transcription profiles of tissue qualifes as a complex system and a low count cutoff was determined by a Ziph graph, in which the log abundance per gene, as measured counts per million (CPM) for all samples, is graphed against the log rank of each gene (Fig. 2). The use of Ziph's law to filter out low expressed genes replaces the application of an arbitrary threshold for gene expression. The requirement that genes be significant at p (adj) ≤ 0.05 in at least one mapping algorithm ensures that only those genes that are highly significant are passed onto the enrichment step.

Data-mining and visualization with cytoscape

Genes with p(adj) ≤ 0.05 in either GMAP or Tophat (SJM) results were passed to Cytoscape (v3.7.1) App ClueGO/CluePedia (v2.5.5) for enrichment and network analyses. Each gene is assigned GO biological process terms (if available) and this information is used to find terms that are enriched in the data. ClueGo parameters used included a two sided-hypergeometric test with an initial cut-off of p(adj) 0.025, corrected with the Bonferroni step down method. Terms were limited to GO levels between 5 and 9 and the kappa score threshold was 0.4. At least three genes per term were required. The GO term fusion GO groups options were selected; these account for the redundancy of GO terms. ClueGO selects GO groups overview terms with the highest significance level (lowest p(adj) value). The log_2 fold-change values were transferred into Cytoscape and
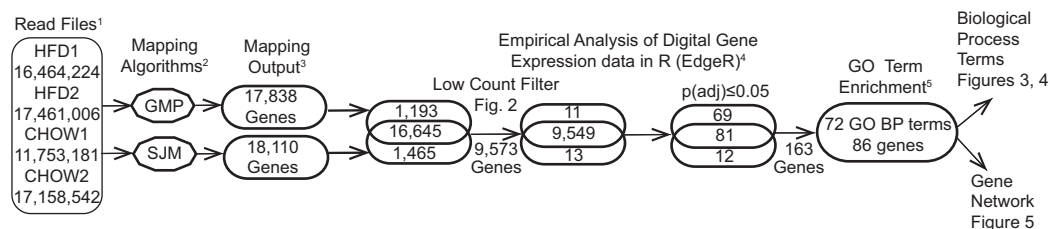
Figure 1 Bioinformatic workflow and results. Details of this workflow are available as supplemental file1.pdf DOI 10.6084/m9.figshare.12037272. (1) Read files are quality-control subjected files from the Illumina IIx. (2) The data was subjected to two mapping programs. (3) The results were quantitated and passed separately to edgeR. (4) The $\log_{10}$CPM data generated in edgeR was used to filter out low counts (supplemental_file_2.xlsx DOI 10.6084/m9.figshare.12037272) and select genes meeting the statistical cutoff of p(adj) ≤ 0.05 (supplemental_file_3.xlsx DOI 10.6084/m9.figshare.12037272). (5) The 163 genes meeting the statistical criteria were subjected to enrichment analysis, resulting in 86 genes that are enriched in 72 GO biological process terms.

displayed as gene node color. Adobe Illustrator (v24.0.1) was used for final mark-up of the networks.

RESULTS & DISCUSSION

The outcome of the bioinformatic workflow is shown in Fig. 1. The process started with over 62.8 million reads and ended with 86 genes with p(adj) ≤ 0.05 that map to 72 GO Biological process terms after enrichment analysis (Fig. 3). Of the 163 genes (Table S1, DOI 10.6084/m9.figshare.12037272) subjected to GO term enrichment, 92 (~58%) are downregulated. Of the 86 retained in the enrichment analysis, 64 (~74%) were downregulated and 22 (~26%) were upregulated in HFD compared to the CHOW condition. The level of nitric oxide synthase (NOS) showed no significant change but Leptin (Lep) was higher in the HFD rats in the physiological data reported for these animals (*Sweazea, Lekic & Walker, 2010*). This corresponds to the RNA-Seq data, in which *eNOS3* (endothelial nitric oxide synthase or nitric oxide synthase 3) gene shows no difference between the treatments but *Lep* is upregulated. GO BP terms were used for enrichment analysis to identify functions responsive to HFD compared to CHOW. The results of EdgeR analysis consisted of 163 differentially regulated genes with functional annotations that were subjected to GO BP term enrichment analysis using the Cytoscape App ClueGO/CluePedia (v 2.5.5). The resulting network consisted of 86 genes and 72 GO terms.

The consolidation of GO BP terms shown in Fig. 4 is based on the experimental protocol. Five overall processes were deemed relevant to aorta, such as vascular processes and muscle remodeling. The high-fat diet treatment induced changes in multiple lipid-related processes, so these terms were consolidated. Changes in genes involved with carbohydrate processes are also correlated to the diet. Hormone signaling, especially insulin and other peptide hormones are also modulated by diet. Although there are significant GO terms that are not connected to others in the network, adding the genes to the network results in a single, interconnected network (Fig. 5). Table 1 lists all genes in the network and their fold-change in HFD aorta as compared to CHOW.
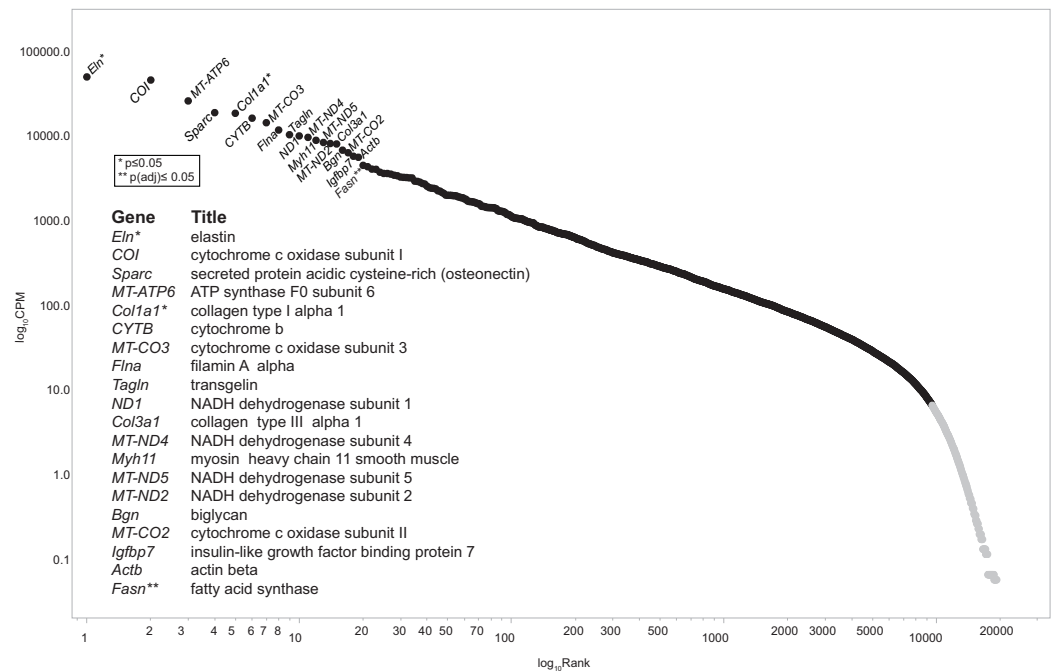
Figure 2 Ziph curve. By plotting the log abundance against the log rank of each gene for all samples, a line with two slopes is obtained. Genes before or near the downturn in slope (black markers) have adequate read coverage for differential expression analyses since an increase in coverage will not change the slope. This eliminates the reliance on estimates of gene length or the assumption that fold-change below an arbitrary level is insignificant. Genes with a $\log_{10}$ CPM ≥ 6.3 (about 100 reads) were selected for further analysis. This retains 9,587 genes out of a total of 19,303 (49.7%) from the consolidated dataset. An interactive version of this graph is available as Fig. S1 (DOI 10.6084/m9.figshare.12037272) Note: the file must be downloaded first and will open in browser.

Recent advances in bioinformatics and methodology for the study of gene expression allow the identification and validation of a growing number of gene targets involved with key biological processes. As such, the goal of this pilot study was to provide a foundation from which to identify potential pathways and signaling intermediates that contribute to vascular dysfunction during early, diet-induced metabolic disease. As hypothesized, HFD-induced metabolic dysfunction altered pro-contractile and pro-inflammatory genes and biological processes associated with vascular dysfunction. The top 20 highest expressed transcripts in all conditions are consistent with that expected for aortic tissue (Fig. 2). *Elas, Col1a1*, and *Col3a1* are highly expressed and produce extracellular matrix (ECM) proteins. *Elas* and *Col1a1* are significant at $p \leq 0.05$, while the ECM protein transcript Col1a2 is differentially regulated at $p(\text{adj}) \leq 0.05$; all are down regulated. Principal biological processes and gene clusters that were stimulated in aortic tissue following the short-term HFD included muscle cell remodeling, vascular functions, as well as insulin/peptide hormone, lipid and carbohydrate processes. There were also several genes associated with circadian rhythm function, including *Nr1d1*, *Per1*, *Noct*, *Nampt*, *Egr1* and *Th*, that were broadly linked to five nodes informed by enrichment analysis and by the experimental protocol. These data highlight the distinct initial gene
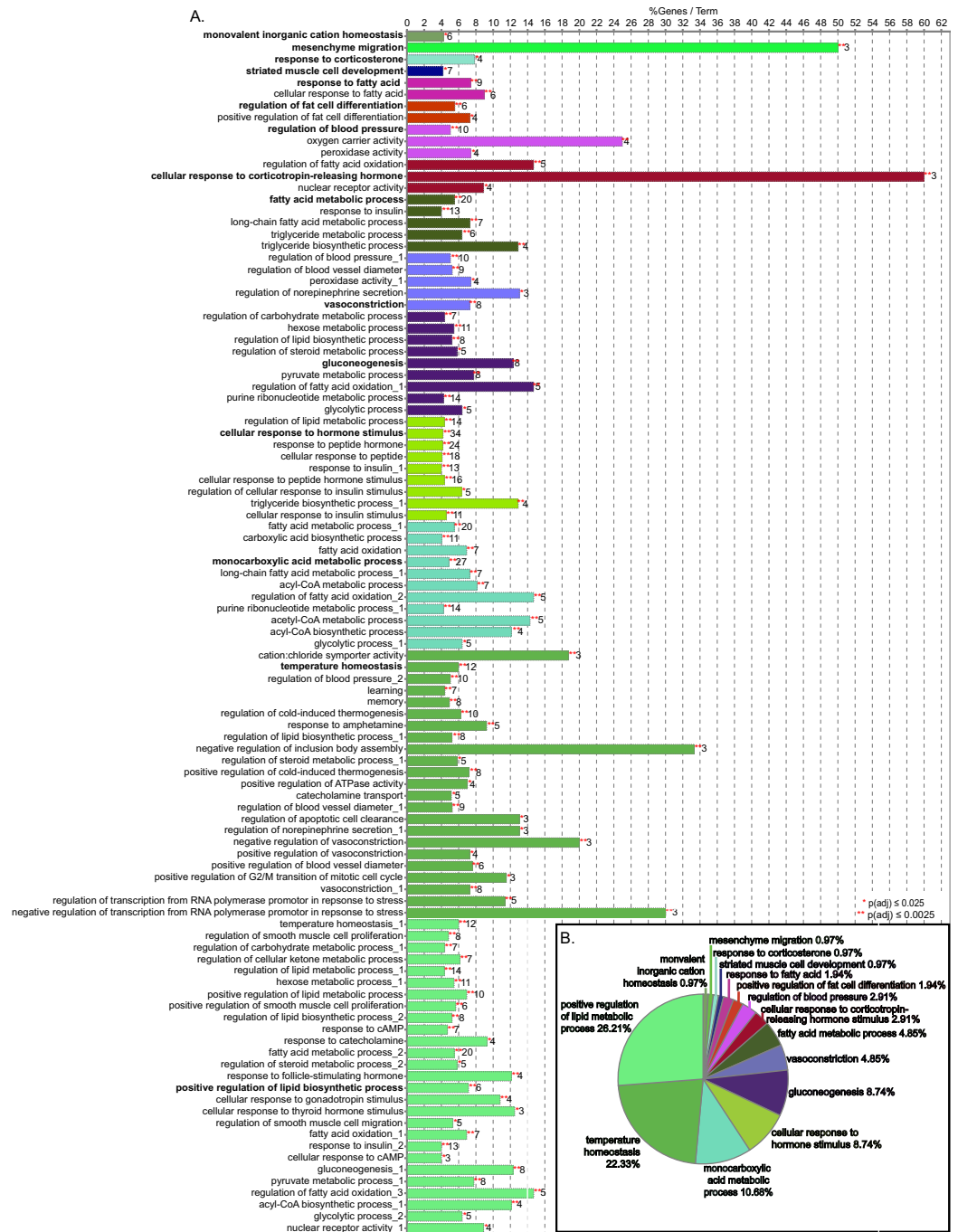
Figure 3 GO biological process term enrichment results. (A) Bar chart indicates the percent of genes represented in the dataset when compared to the total number of genes linked to GO term. The number of genes in this data that share the GO term shown at the end of the bar. The terms are clustered by related functions and are indicated by color, the overview term for each cluster is bolded. There are 72 terms, but some terms are in more than one cluster, these are indicated by numbers after the title. (B) Pie chart indicated the proportion of genes associated with overview terms.
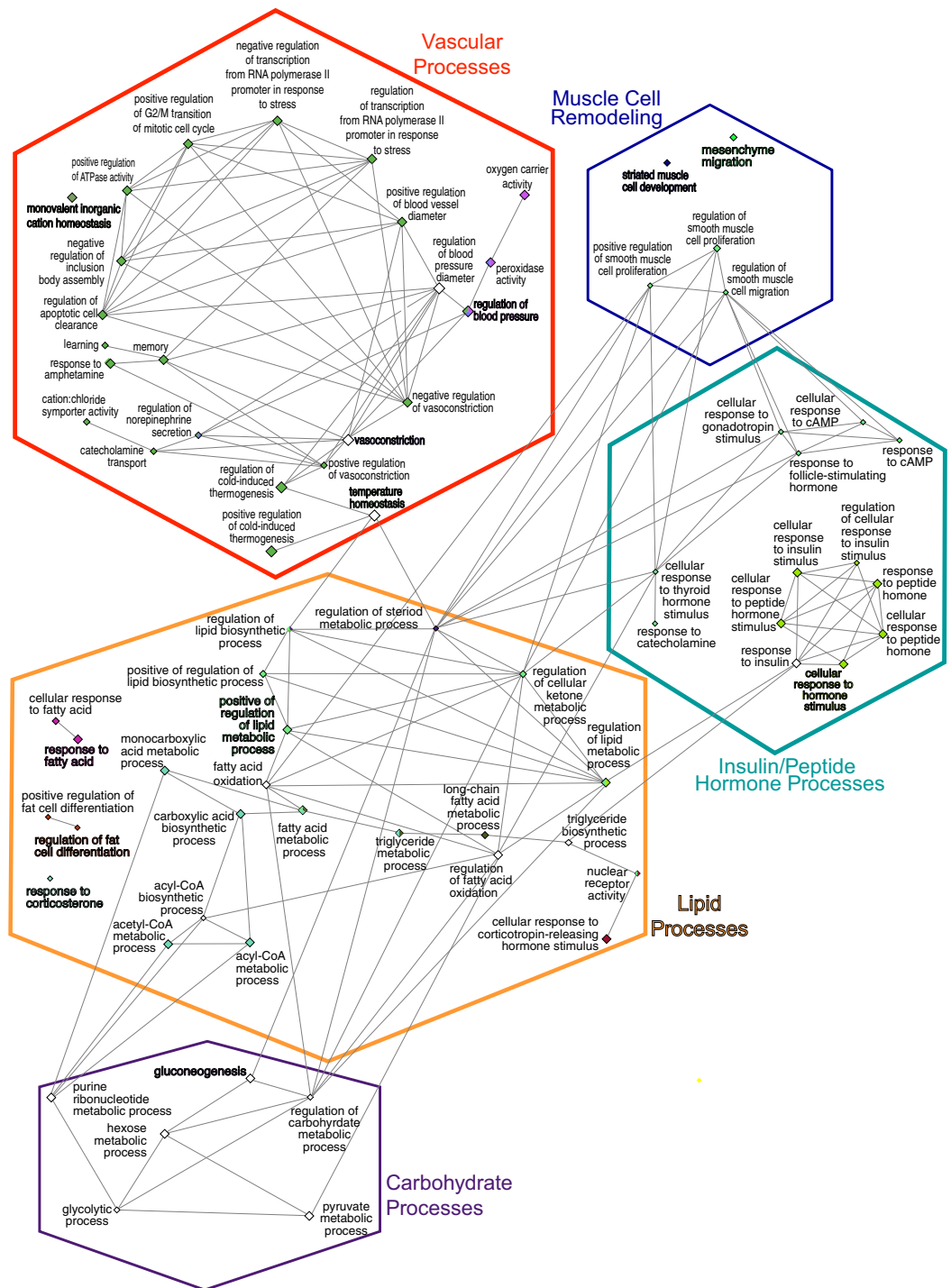
Figure 4 GO Biological Process network. Overview terms are based on the most significant term (Fig. 3) within the grouping and are indicated by bold color text. The edges connecting the nodes are term to term interactions. Nodes with multiple colors are assigned to multiple clusters. The size of the node indicates significance, all are p(adj) ≤ 0.025. Larger nodes are more significant because they are higher-level terms in the GO hierarchy, so they include more processes and hence, more genes (Fig. 3A). The hexagons are the groupings based upon the experimental protocol used in the present study and correspond to the nodes in Fig. 5.
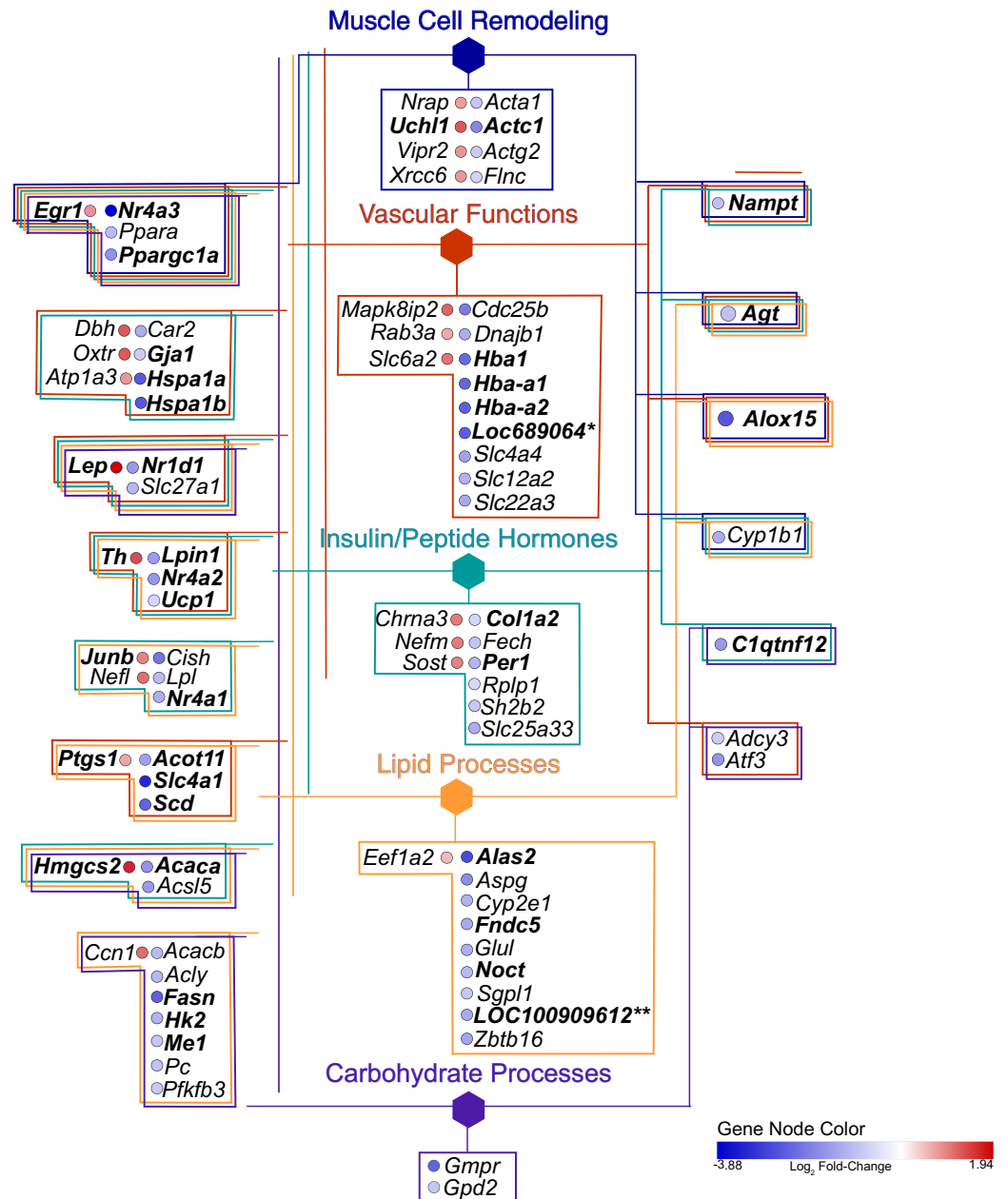
Figure 5 Gene network. Hexagonal nodes are the groupings shown in Fig. 4, round nodes are genes. Table 1 are the abbreviations for all genes in this network, bolded gene names are discussed in this paper. Genes in frames have are linked to the same processes. *LOC287167** is an alpha-globin gene and *LOC100909612*** is an uncoupling-like protein.

expression profiles and alteration of associated biological processes of the aortic wall during early metabolic dysfunction. Moreover, diet during early life appears to be a strong determinant of vascular dysfunction. The physiological relevance of notable genes and their linkage to the five processes shown in Figs. 4 and 5 are discussed below.

Table 1 Key to Figure 5 gene symbols.

Gene symbol	Title	logFC
Acaca	**Acetyl-CoA carboxylase 1**	**−1.6**
Acacb	Acetyl-CoA carboxylase beta	−1.0
Acly	ATP citrate lyase (Acly) transcript variant	−1.1
Acot11	Acyl-CoA thioesterase 11	−1.4
Acsl5	Long-chain-fatty-acid-CoA ligase 5	−1.5
Acta1	Actin alpha 1 skeletal muscle	−0.9
Actc1	**Actin alpha cardiac muscle 1**	**−1.8**
Actg2	Actin gamma 2 smooth muscle enteric	−0.8
Adcy3	Adenylate cyclase 3	−0.8
Agt	Angiotensinogen (serpin peptidase inhibitor clade A member 8)	−1.0
Alas2	**Aminolevulinate delta-synthase 2**	**−2.7**
Alox15	**Arachidonate 15-lipoxygenase**	**−2.6**
Aspg	Asparaginase homolog (*S. cerevisiae*)	−1.7
Atf3	Activating transcription factor 3	−1.6
Atp1a3	ATPase Na+/K+ transporting alpha 3 polypeptide	0.8
C1qtnf12	C1q and TNF related 12	−1.6
Car2	Carbonic anhydrase 2	−1.2
Cdc25b	Cell division cycle 25B	−2.0
Chrna3	Cholinergic receptor nicotinic alpha 3 (neuronal)	1.0
Cish	Cytokine inducible SH2-containing protein	−2.1
Col1a2	Collagen, type I, alpha 2	−0.6
Cyp1b1	Cytochrome P450 family 1 subfamily b polypeptide 1	−1.3
Cyp2e1	Cytochrome P450 family 2 subfamily e polypeptide 1	−1.2
Cyr61	Cysteine-rich angiogenic inducer 61	1.1
Dbh	Dopamine beta-hydroxylase (dopamine beta-monooxygenase)	1.3
Dnajb1	DnaJ (Hsp40) homolog subfamily B member 1	−1.2
Eef1a2	Eukaryotic translation elongation factor 1 alpha 2	0.5
Egr1	**Early growth response 1**	**0.8**
Fasn	**Fatty acid synthase**	**−2.4**
Fech	Ferrochelatase	−0.9
Flnc	Filamin C gamma	−0.7
Fndc5	**Fibronectin type III domain containing 5**	**−1.3**
Gja1	**Gap junction protein alpha 1**	**−0.7**
Glul	Glutamate-ammonia ligase	−1.2
Gmpr	Guanosine monophosphate reductase	−2.4
GPD2	Glycerol-3-phosphate dehydrogenase mitochondrial	−0.9
Hba1	**Hemoglobin alpha 1**	**−2.3**
Hba2	**Hemoglobin alpha 2**	**−2.5**
Hbb-b1	**Hemoglobin beta adult major chain**	**−2.5**
Hk2	**Hexokinase 2 (Hk2)**	**−1.2**
Hmgcs2	**3-hydroxy-3-methylglutaryl-CoA synthase 2 (mitochondrial)**	**1.7**
Hspa1a	**Heat shock 70kD protein 1A**	**−2.5**
Hspa1b	**Heat shock 70kD protein 1B**	**−2.5**

(Continued)

Gene symbol	Title	logFC
Junb	Jun B proto-oncogene	0.9
Lep	**Leptin**	**1.9**
LOC100909612	**Mitochondrial brown fat uncoupling protein 1-like**	**−1.3**
LOC287167	**Globin alpha**	**−2.3**
Lpin1	Lipin 1	−1.5
Lpl	Lipoprotein lipase	−1.1
Mapk8ip2	Mitogen-activated protein kinase 8 interacting protein 2	1.2
Me1	**Malic enzyme 1 NADP(+)-dependent cytosolic**	**−0.9**
Nampt	**Nicotinamide phosphoribosyltransferase**	**−1.0**
Nefl	Neurofilament light polypeptide	1.1
Nefm	Neurofilament medium polypeptide	1.0
Noct	**Nocturnin**	**−1.1**
Nr1d1	**Nuclear receptor subfamily 1 group D member 1**	**−1.5**
Nr4a1	**Nuclear receptor subfamily 4 group A member 1**	**−1.2**
Nr4a2	**Nuclear receptor subfamily 4 group A member 2**	**−1.6**
Nr4a3	**Nuclear receptor subfamily 4 group A member 3**	**−3.9**
Nrap	Nebulin-related anchoring protein (Nrap) transcript variant 1	0.7
Oxtr	Oxytocin receptor	1.3
Pc	Pyruvate carboxylase	−0.9
Per1	**Period circadian clock 1**	**−1.1**
Pfkfb3	6-phosphofructo-2-kinase/fructose-2 6-biphosphatase 3	−0.8
Ppara	Peroxisome proliferator activated receptor alpha	−1.0
Ppargc1a	**Peroxisome proliferator-activated receptor gamma coactivator 1 alpha**	**−1.7**
Ptgs1	Prostaglandin-endoperoxide synthase 1	0.7
Rab3a	RAB3A member RAS oncogene family	0.6
Rplp1	Ribosomal protein large P1	−0.6
Scd1	**Stearoyl-Coenzyme A desaturase 1**	**−2.4**
Sgpl1	Sphingosine-1-phosphate lyase 1	−0.9
Sh2b2	SH2B adaptor protein 2	−0.9
Slc12a2	Solute carrier family 12 (sodium/potassium/chloride transporter)	−1.2
Slc22a3	Solute carrier family 22 (organic cation transporter) member 3	−0.8
Slc25a33	Solute carrier family 25 (pyrimidine nucleotide carrier) member 33	−1.3
Slc27a1	Solute carrier family 27 (fatty acid transporter) member 1	−1.1
Slc4a1	**Solute carrier family 4 (anion exchanger) member 1**	**−3.3**
Slc4a4	Solute carrier family 4 sodium bicarbonate cotransporter member 4	−1.4
Slc6a2	Solute carrier family 6 (neurotransmitter transporter) member 2	1.1
Sost	Sclerostin	1.0
Th	**Tyrosine hydroxylase**	**1.4**
Uchl1	**Ubiquitin carboxyl-terminal esterase L1 (ubiquitin thiolesterase)**	**1.3**
Ucp1	**Uncoupling protein 1 (mitochondrial proton carrier)**	**−0.6**
Vipr2	Vasoactive intestinal peptide receptor 2	0.8
Xrcc6	X-ray repair complementing defective repair in Chinese hamster cells 6	0.8

Note:

This table lists the gene symbols and corresponding genes that were detected in the aorta samples in addition to their log fold change (logFC). Bolded entries are genes discussed in the text.

Muscle cell remodeling

Our analysis identified 17 (~19%) genes related to muscle cell remodeling with a number of these genes associated with processes involving the regulation of smooth muscle proliferation and mesenchyme migration. While expression of the majority of these genes were consistent with the negative alterations in vascular dysfunction, these findings were notable given the brevity of the dietary intervention, age of the animals, and time-course for muscle cell remodeling in vascular diseases. Reduced expression of *Actc1* parallels findings that occur during the onset of heart disease through induction of cardiomyocyte apoptosis (*Jiang et al., 2010*) and increased expression of *Uchl1*, part of the ubiquitin-proteasome system associated with muscle atrophy in diabetic rats (*Reddy et al., 2018*). Further, *Nr4a3* was downregulated, which is a transcription factor connected to all five of the main biological functions included in our analysis. *Nr4a3* is a transcriptional target of p53, triggering apoptosis and playing a suppressive role in cancer (*Fedorova et al., 2019*). While the aorta was analyzed in the present research, previous studies in rats suggest the decreased expression of *Nr4a3* may be associated with reduced signaling for metabolic capacity in muscle (*Oita et al., 2009*; *Pearen et al., 2012*).

Vascular functions

Genes associated with vascular function were abundant and included terms in the GO biological process network related to the regulation of blood pressure, vasoconstriction, temperature homeostasis, regulation of apoptotic cell clearance, and oxygen carrier activity (Figs. 3 and 4). In addition, many of the genes associated with monovalent inorganic anion homeostasis were downregulated, including *Slc4a1*. This encoded protein mediates an electroneutral chloride/bicarbonate exchange in physiological conditions and is the main membrane protein in vertebrate erythrocytes (*Barneaud-Rocca, Etchebest & Guizouarn, 2013*). In addition, Slc4a1 plays a role in signaling aged cells for clearance through macrophage-mediated phagocytosis (*Badior & Casey, 2018*). Relatedly, genes involved in oxygen carrier activity displayed reduced expression, including *Hba1*, *Hba-a2*, *Hbb-b1*, and *Loc689604*, a novel hemoglobin alpha gene. Recent studies in human and mice tissue have found hemoglobin alpha subunit expression in blood vessel walls, where it appears to localize at the myoendothelial junction and plays a role in regulating nitric oxide signaling between endothelium and smooth muscle (*Butcher et al., 2014*). Decreases in associated gene expression in the current study is suggestive of vascular dysfunction, perhaps through reduced nitric oxide signaling. This finding is corroborated with previous physiological data from these HFD animals, that exhibited impaired endothelium-dependent vasodilation (*Sweazea, Lekic & Walker, 2010*; *Sweazea & Walker, 2011*).

Egr1 functions as a master transcriptional switch activated by ischemia to trigger expression of pivotal regulators of inflammation, coagulation, and vascular hyperpermeability (*Silverman & Collins, 1999*; *Yan et al., 2000*) and was upregulated. Although ischemic tissue damage was not directly assessed in the present study, *Erg1* activation is a notable finding considering its central role in the pathogenesis of vascular dysfunction (*Yan et al., 2000*). Therefore, this finding may be suggestive of early tissue damage occurring in the aortic wall of the HFD animals. Another intriguing finding was

the decreased expression of *Nampt* (aka *Visfatin*). *Nampt* is the rate limiting component in the mammalian nicotinamide adenine dinucleotide (NAD) biosynthesis pathway and connects NAD-dependent sirtuin signaling, constituting a strong intrinsic defense system against various stresses (*Wang & Miao, 2015*). In the present study, we show a significant decrease in *Nampt* expression in aortic tissue potentially implicating this gene as nutrient-sensitive to the HFD treatment. Together the expression profile of vascular function related genes highlight potential negative alterations occurring in aortic tissue during the early stages of metabolic dysfunction, which are consistent with the impaired endothelium-mediated vasodilation observed in prior studies of ex vivo small resistance arteries from these animals (*Sweazea & Walker, 2011*; *Sweazea & Walker, 2012*).

Insulin/peptide hormones

The adipokine encoding gene, *Lep*, displayed increased expression paralleling the elevated leptin levels in an obesogenic state (*Pan, Guo & Su, 2014*). In rats, leptin has been reported to stimulate the proliferation and migration of vascular smooth muscle cells in the aorta, implying leptin may play a role in the formation and development of vascular remodeling (*Oda, Taniguchi & Yokoyama, 2001*). Leptin appears to directly stimulate cellular hypertrophy via p38 MAP kinase in rat vascular smooth muscle cells (*Shin et al., 2005*). In fact, leptin receptors are present in endothelial cells providing a target for leptin action on the vascular wall (*Fortuño et al., 2002*).

Hspa1a and *Hspa1b* encode for heat shock proteins that are major orchestrators of the cellular stress response associated with several human diseases (*Daugaard, Rohde & Jäättelä, 2007*; *McCallister et al., 2015*; *Richter, Haslbeck & Buchner, 2010*). Both are down regulated in the HFD samples. *Hspa1a* overexpression protects many cell types against a wide variety of stresses, including hypoxia and reoxygenation injury (*Hutter et al., 1994*; *Radford et al., 1996*). Indeed, elevated Hspa1a has been reported to provide cardioprotection against ischemia-reperfusion induced myocardial infarction and apoptosis (*Quindry et al., 2007*). Whereas low levels of intracellular and circulating Hspa1a promote a proinflammatory state and increase the vulnerability of the arterial wall to the damaging action of vascular risk factors involved in endothelial dysfunction—the first stage in the development of the atherosclerotic plaque (*Dulin, García-Barreno & Guisasola, 2012*). The role of *Hspa1b* in the vasculature is less apparent and, although closely related to *Hspa1a*, it is distinct and has remained conserved in a lineage preceding placental mammals (*Hess et al., 2018*). Therefore, selection may be acting to preserve not only the primary function but also other less well-studied secondary functions of the molecules, like lipid binding and cell signaling (*Hess et al., 2018*). *Gja1* (connexin) was downregulated and similar to *Hspa1a* and *Hspa1b* is associated with both vascular functions and insulin/peptide hormones. *Gja1* encodes the protein connexin 43, a gap junction protein important in cell-to-cell communication and in vascular myoendothelial gap junctions in the heart and other tissues (*Triggle et al., 2012*; *Xu et al., 2017*). In diabetic vascular disease where blood glucose levels are both elevated and not well controlled, advanced glycation end products (AGEs) may also impact both the expression and function of connexins, and thus, contribute to the development of endothelial dysfunction and vascular disease (*Wang et al., 2011*).

Lipid processes

Similar to the pattern noted with insulin/peptide hormone process, there was an expected decrease in genes encoding for enzymes involved in fatty acid biosynthesis. Of these, *Fasn* and *Acaca* encode enzymes in the fatty acid synthesis pathway and are well-known to increase with rising insulin levels associated with elevated carbohydrate intake (*Saltiel & Kahn, 2001*; *Wong & Sul, 2010*). Beyond the high level of saturated fat and low carbohydrate consumed by the HFD rats in the present study, the downregulation of these genes may also be related to increased oxidative stress, which has been noted to down regulate intermediates in the insulin signaling pathway and promote insulin resistance (*Bloch-Damti & Bashan, 2005*; *Fridlyand & Philipson, 2006*; *Hurrle & Hsu, 2017*). In relation, the HFD rats showed significant increases in circulating thiobarbituric acid reactive substances (TBARS) as well as vascular oxidative stress as measured by DCF fluorescence (*Sweazea & Walker, 2011*). In addition, they developed significantly impaired vasodilation in the mesenteric arteries that was mediated by oxidative stress (*Sweazea & Walker, 2012*).

Another important finding was the decreased expression of genes associated with brown adipose tissue (BAT). *Fndc5* gene was reduced in HFD rats. The encoded protein from *Fndc5* is a precursor to irisin which reportedly acts on white adipose cells to stimulate uncoupling protein expression and brown-fat-like development (*Boström et al., 2012*). In relation, we report decreased expression *Ucp1* and of LOC100909612, annotated as encoding a potential Upc1-Like protein. Also decreased was *Acot11*, which catalyze the hydrolysis of fatty acyl-CoA thioesters and is enriched in BAT (*Cohen, 2013*). *Acot11* also appears to regulate the availability of substrates for beta-oxidation and uncoupling (*Han & Cohen, 2012*; *Okada et al., 2016*; *Zhang et al., 2012*). While there is a reduction in BAT in humans with increased obesity and metabolic dysfunction (*Franssens et al., 2017*), the decreased expression of these BAT genes in the aortic wall from the present study was an unexpected finding. This may have been due to remnants of perivascular adipose tissue (PVAT), the adipose tissue surrounding blood vessels, in our tissue samples. PVAT shares several of the defining characteristics of BAT, including its cellular morphology and expression of thermogenic genes characteristic of brown adipocytes (*Hildebrand, Stümer & Pfeifer, 2018*). Moreover, PVAT is the source of several paracrine factors that regulate vascular tone (*Chang et al., 2012*; *Friederich-Persson et al., 2017*).

Carbohydrate processes

There was a general decrease in genes related to the regulation of carbohydrate metabolic processes including *Hk2*, which phosphorylates glucose to produce glucose-6-phosphate and is regulated in part by insulin (*Osawa et al., 1995*; *Okada et al., 2016*). Development of diabetes is associated with a shift in cardiac glucose metabolism including significant decreases in *Hk2* content (*Calmettes et al., 2015*). The general downregulation in the insulin signaling pathway is notable as HFD rats display several features of metabolic dysfunction including hyperglycemia, impaired glucose tolerance, oxidative stress as well as oxidative-stress mediated vascular dysfunction (*Sweazea, Lekic & Walker, 2010*; *Sweazea & Walker, 2011*; *Sweazea & Walker, 2012*). Because the vasculature is located at

the interface between blood and tissue, vessel walls are particularly exposed to this oxidative stress and may experience negative alterations in insulin signaling before other tissues (*Wiernsperger, 2003*).

Other considerations

In the present study, the number of genes associated with circadian function is suggestive of biological crosstalk between circadian rhythm and metabolism in the vasculature. Specifically, there was a notable decrease in expression of genes related to circadian function, including *Nr1da1* (a.k.a. Rev-ERBA), *Per1*, *Noct*, and *Nampt*. In addition, the increase in *Lep* mentioned previously is intriguing given that leptin has been reported to affect circadian rhythm in mammals (*Prosser & Bergeron, 2003*). The relationship between the circadian clock and these genes along with their related metabolic pathways may represent a novel target for studying the pathogenesis of vascular diseases. Disruption of daily rhythms with a chronic HFD in mice has been found to be rapidly reversible in liver tissue (via PERIOD2:LUCIFERASE bioluminescence rhythm) (*Branecky, Niswender & Pendergast (2015)*). Though, it is unclear if this would be similar in the vasculature. In relation, time-restricted feeding in alignment with light and dark cycles has been found to partially restore day-night differences in cardiac remodeling, triglyceride synthesis, lipidome, and metabolic flexibility in mice (*Mia et al., 2021*). Therefore, future work should investigate HFD cessation, as well as time-restricted feeding models on circadian-related genes in the vasculature. Though this would be complex as the number of animals required, the appropriate time series of sample collection, and selection of vasculature tissue location throughout the cardiovascular system is not fully apparent. Indeed, circadian clock components display differences in expression and localization throughout the cardiovascular system, which may confer nuances of circadian clock signaling in a cell-specific manner (*Anea et al., 2018*).

In rodents, high fat feeding has been reported to alter circadian synchronization to light (*Mendoza, Pévet & Challet, 2008*), and obesity reduces circadian gene expression in concert with impaired endothelial function in the aorta (*Nernpermpisooth et al., 2015*). Two core clock genes, *Per1* and *Nrd1d*, were downregulated in the aorta of rats on the HFD; both are transcriptional repressors. *Per1* is reportedly decreased in vascular smooth muscle in type 2 diabetic *db/db* mice (*Su et al., 2012*). Rev-ERBA can reversibly bind to heme, which changes its interaction with other clock components (*Yin et al., 2007*). In the present study, the enzyme responsible for the rate-limiting step in Heme production, *Alas1*, was downregulated. The role of heme availability in circadian signaling and metabolic dysfunction are unresolved. NAMPT catalyzes the rate limiting step in the NAD salvage pathway and is also a clock-controlled gene (*Bass & Lazar, 2016*). *Nampt*-dependent oscillatory production of NAD regulates oscillation of clock target gene expression by releasing the core clock component: Clock-Arntl/Bmal1 heterodimer from NAD-dependent Sirt1-mediated suppression (*Ramsey et al., 2009*). *Noct* is another mitochondrial enzyme also under the control of the circadian clock, it catalyzes the dephosphorylation of NADP+ and NADPH. In contrast, *Egr1* was increased. *Egr1* appears to play a potential role in the regulation of the hepatic circadian clock in response to
feeding/fasting (*Tao et al., 2015*). The role of *Th* expression in peripheral clocks remains to be elucidated. This provides evidence for the disruption of circadian pathways in aorta are induced by HFD, but the nature of changes remains to be determined. Furthermore, it is not clear if females would respond in a similar fashion. In fact, the response may very well be different in females as the effect of HFDs on the circadian rhythm display some notable dependence on biological sex. For instance, in female mice estradiol has been reported to regulate the daily rhythms underlying diet-induced obesity (*Omotola et al., 2019*). Ovarian hormones in female mice provide a protective circadian mechanism, preventing disruption of daily rhythms from high-fat feeding (*Palmisano, Stafford & Pendergast, 2017*). Though the age of mice is an important determinant of this response since a HFD has been noted to alter circadian genes in mammary glands of female mice during puberty (*Sundaram, Johnson & Yan, 2020*). These mice were the same age as the adolescent male rats used in the present study (6-weeks), therefore, future work should consider female animals in the context of puberty, as well as menopause. Such research may better delineate the putative role of estrogen as a protective agent against HFD-induced circadian disruption.

The current study has some limitations. Due to the nature of tissue extraction and the limited number of samples, it was not possible to assess time-related changes in gene expression leading to vascular dysfunction. Therefore, significant changes may have occurred at earlier or later time points. Another important aspect relates to the HFD diet used in the present rodent model. These rats were not genetically prone to develop atherosclerotic lesions, therefore the diet is likely unable to induce significant vascular disease. However, our previous work showed impaired function in these animals (*Sweazea, Lekic & Walker, 2010*; *Sweazea & Walker, 2011*). A third limitation of the present study was the small sample size in each group, although this is typical of sequencing studies of this nature as evidenced by similar sample sizes reported in other research (*Bao et al., 2016*; *Xi et al., 2017*). As a pilot study, this work is intended to inform future research efforts in this area, with larger samples. We acknowledge that the generated statistics and described effects could be within normal biological variation and need to be replicated with larger scaled research. Such research has been performed in other animal models, including a 12-month HFD study in adult pigs (*Milenkovic et al., 2020*), however this study and others investigating the vasculature have used microarray gene assessments (*Bao et al., 2016*). The technological platform employed is not trivial as microarray analysis may induce a more biased view of gene expression and does not allow the whole transcriptome to be assayed in comparison to RNA-seq (*Rao et al., 2019*). Importantly, the study was able to demonstrate that RNA-seq has the sensitivity to detect differences in gene expression in the given the experimental protocol. Another point to emphasize is that this data validates several findings established in the physiological literature (e.g., involvement of circadian clocks) and experimentally (e.g., the increased circulating leptin levels, hypertension and impaired vasodilation previously observed in these animals). It is important to note that gene expression data is a proxy for active protein concentrations. As such, there are four principles of data mining using GO terms that are important to understand its potentials and weaknesses. First, differential gene expression data is a direct

measure of events in the nucleus. Although an mRNA template is required to produce proteins, it is subjected to post-transcriptional control and subsequent proteins require post-translational modifications, so mRNA-based assays are a proxy for fully active protein. Second, transcripts from the same gene may code for multiple proteins, some of which act in a tissue-specific manner. An example of this in Figs. 3A and 4 are the inclusion of the GO terms 'memory' and 'learning;' these terms reflect the role in the nervous system. GO term enrichment alone does not take into account the tissue and experimental protocol. Third, by their nature, gene ontologies are complex, and this is reflected by the redundancy in networks of GO terms. For example, vasoconstriction is an overview term that 4.85% of the 86 genes share, and both the negative and positive regulation of vasoconstriction are included as GO BP terms since these processes involve the same genes. The inclusion of multiple levels of GO terms (in this case 5–9) is necessary to capture an optimized subset of genes. Thus, any conclusions regarding specific gene products will need to be empirically validated.

CONCLUSION

The current body of literature has placed emphasis on examining the vasculature in models of advanced metabolic dysfunction. However, by the time of diagnosis, individuals may already demonstrate a significant vascular burden and disease progression that may limit treatment options. In this pilot study we sought to identify the early effects of HFD on vascular gene expression in the aorta of male adolescent rats using an expansive RNA-Seq approach. Overall, the expression profiles of HFD compared to CHOW displayed genes and pathways that are known to be associated with metabolic derangement and vascular dysfunction. These include processes involving vascular function and muscle remodeling, which are directly relevant to aorta. In addition, the high-fat diet treatment induced changes in multiple lipid-related processes as well as genes involved with carbohydrate processes. Hormone signaling, especially insulin and other peptide hormone-related genes also appeared to be modulated by HFD. Uniquely, several genes involved in BAT development and circadian rhythm displayed altered expression, suggestive of negative alterations in these processes. In conclusion, these results contribute to our molecular understanding of the development of vascular dysfunction in the aorta as a result of a fat-rich diet.

Funding

This project was supported by grants from the National Center for Research Resources (5P20RR016480-12) and the National Institute of General Medical Sciences (8 P20 GM103451-12) from the National Institutes of Health. There was no additional external funding received for this study. The funders had no role in study design, data collection and analysis, decision to publish, or preparation of the manuscript.

Grant Disclosures

The following grant information was disclosed by the authors:
National Center for Research Resources: 5P20RR016480-12.
National Institute of General Medical Sciences: 8 P20 GM103451-12.

Competing Interests

Alex E. Mohr is employed by Isagenix International LLC. Isagenix was not involved in any aspect of the study. All authors have no financial interests regarding the outcomes of this investigation. All other authors declare no conflict of interests.

Author Contributions

- Alex E. Mohr analyzed the data, prepared figures and/or tables, authored or reviewed drafts of the paper, and approved the final draft.
- Rebecca A. Reiss conceived and designed the experiments, performed the experiments, analyzed the data, prepared figures and/or tables, authored or reviewed drafts of the paper, and approved the final draft.
- Monique Beaudet performed the experiments, authored or reviewed drafts of the paper, and approved the final draft.
- Johnny Sena performed the experiments, authored or reviewed drafts of the paper, and approved the final draft.
- Jay S. Naik conceived and designed the experiments, authored or reviewed drafts of the paper, and approved the final draft.
- Benjimen R. Walker conceived and designed the experiments, authored or reviewed drafts of the paper, donated the tissues used for the analyses from the ongoing study, and approved the final draft.
- Karen L. Sweazea conceived and designed the experiments, performed the experiments, analyzed the data, authored or reviewed drafts of the paper, and approved the final draft.

Animal Ethics

The following information was supplied relating to ethical approvals (i.e., approving body and any reference numbers):

Animal care procedures were reviewed and approved by the Institutional Animal Care and Use Committee of the University of New Mexico School of Medicine (AAALAC # 000222).

Data Availability

The raw data are available at the Gene Expression Omnibus (GEO): GSE147335.

REFERENCES

Adamic L. 2011. Complex systems: unzipping Zipf's law. *Nature* **474(7350)**:164–165 DOI 10.1038/474164a.

Altschul SF, Gish W, Miller W, Myers EW, Lipman DJ. 1990. Basic local alignment search tool. *Journal of Molecular Biology* **215(3)**:403–410 DOI 10.1016/S0022-2836(05)80360-2.

Anders S, Pyl PT, Huber W. 2015. HTSeq—a Python framework to work with high-throughput sequencing data. *Bioinformatics* **31(2)**:166–169 DOI 10.1093/bioinformatics/btu638.

Andrews S. 2010. FastQC: A quality control tool for high throughput sequence data. *Available at http://www.bioinformatics.babraham.ac.uk/projects/fastqc/*.

Anea CB, Merloiu AM, Fulton DJR, Patel V, Rudic RD. 2018. Immunohistochemistry of the circadian clock in mouse and human vascular tissues. *Vessel Plus* **2(7)**:16 DOI 10.20517/2574-1209.2018.46.

Badior KE, Casey JR. 2018. Molecular mechanism for the red blood cell senescence clock. *IUBMB Life* **70(1)**:32–40 DOI 10.1002/iub.1703.

Bao MH, Luo HQ, Chen LH, Tang L, Ma KF, Xiang J, Dong LP, Zeng J, Li GY, Li JM. 2016. Impact of high fat diet on long non-coding RNAs and messenger RNAs expression in the aortas of ApoE(-/-) mice. *Scientific Reports* **6(1)**:34161 DOI 10.1038/srep34161.

Barneaud-Rocca D, Etchebest C, Guizouarn H. 2013. Structural model of the anion exchanger 1 (SLC4A1) and identification of transmembrane segments forming the transport site. *Journal of Biological Chemistry* **288(37)**:26372–26384 DOI 10.1074/jbc.M113.465989.

Bass J, Lazar MA. 2016. Circadian time signatures of fitness and disease. *Science* **354(6315)**:994–999 DOI 10.1126/science.aah4965.

Benjamin EJ, Muntner P, Alonso A, Bittencourt MS, Callaway CW, Carson AP, Chamberlain AM, Chang AR, Cheng S, Das SR, Delling FN, Djousse L, Elkind MSV, Ferguson JF, Fornage M, Jordan LC, Khan SS, Kissela BM, Knutson KL, Kwan TW, Lackland DT, Lewis TT, Lichtman JH, Longenecker CT, Loop MS, Lutsey PL, Martin SS, Matsushita K, Moran AE, Mussolino ME, O'Flaherty M, Pandey A, Perak AM, Rosamond WD, Roth GA, Sampson UKA, Satou GM, Schroeder EB, Shah SH, Spartano NL, Stokes A, Tirschwell DL, Tsao CW, Turakhia MP, VanWagner LB, Wilkins JT, Wong SS, Virani SS. 2019. Heart Disease and Stroke Statistics-2019 update: a report from the American Heart Association. *American Heart Association Council on Epidemiology and Prevention Statistics Committee and Stroke Statistics Subcommittee* **139(10)**:e56–e66 DOI 10.1161/CIR.0000000000000659.

Bindea G, Mlecnik B, Hackl H, Charoentong P, Tosolini M, Kirilovsky A, Fridman WH, Pagès F, Trajanoski Z, Galon J. 2009. ClueGO: a Cytoscape plug-in to decipher functionally grouped gene ontology and pathway annotation networks. *Bioinformatics* **25(8)**:1091–1093 DOI 10.1093/bioinformatics/btp101.

Bloch-Damti A, Bashan N. 2005. Proposed mechanisms for the induction of insulin resistance by oxidative stress. *Antioxidants & Redox Signaling* **7(11–12)**:1553–1567 DOI 10.1089/ars.2005.7.1553.

Boström P, Wu J, Jedrychowski MP, Korde A, Ye L, Lo JC, Rasbach KA, Boström EA, Choi JH, Long JZ, Kajimura S, Zingaretti MC, Vind BF, Tu H, Cinti S, Højlund K, Gygi SP, Spiegelman BM. 2012. A PGC1-α-dependent myokine that drives brown-fat-like development of white fat and thermogenesis. *Nature* **481(7382)**:463–468 DOI 10.1038/nature10777.

Branecky KL, Niswender KD, Pendergast JS. 2015. Disruption of daily rhythms by high-fat diet is reversible. *PLOS ONE* **10(9)**:e0137970 DOI 10.1371/journal.pone.0137970.

Butcher JT, Johnson T, Beers J, Columbus L, Isakson BE. 2014. Hemoglobin α in the blood vessel wall. *Free Radical Biology and Medicine* **73**:136–142 DOI 10.1016/j.freeradbiomed.2014.04.019.

Calmettes G, Ribalet B, John S, Korge P, Ping P, Weiss JN. 2015. Hexokinases and cardioprotection. *Journal of Molecular and Cellular Cardiology* **78(Suppl. 1)**:107–115 DOI 10.1016/j.yjmcc.2014.09.020.

Chagoyen M, Pazos F. 2010. Quantifying the biological significance of gene ontology biological processes-implications for the analysis of systems-wide data. *Bioinformatics* **26(3)**:378–384 DOI 10.1093/bioinformatics/btp663.

Chang L, Villacorta L, Li R, Hamblin M, Xu W, Dou C, Zhang J, Wu J, Zeng R, Chen YE. 2012. Loss of perivascular adipose tissue on peroxisome proliferator-activated receptor-γ deletion in smooth muscle cells impairs intravascular thermoregulation and enhances atherosclerosis. *Circulation* **126(9)**:1067–1078 DOI 10.1161/CIRCULATIONAHA.112.104489.

Cline MS, Smoot M, Cerami E, Kuchinsky A, Landys N, Workman C, Christmas R, Avila-Campilo I, Creech M, Gross B, Hanspers K, Isserlin R, Kelley R, Killcoyne S, Lotia S, Maere S, Morris J, Ono K, Pavlovic V, Pico AR, Vailaya A, Wang PL, Adler A, Conklin BR, Hood L, Kuiper M, Sander C, Schmulevich I, Schwikowski B, Warner GJ, Ideker T, Bader GD. 2007. Integration of biological networks and gene expression data using Cytoscape. *Nature Protocols* **2(10)**:2366–2382 DOI 10.1038/nprot.2007.324.

Cohen DE. 2013. New players on the metabolic stage: how do you like them acots? *Adipocyte* **2(1)**:3–6 DOI 10.4161/adip.21853.

Crawford M, Whisner C, Al-Nakkash L, Sweazea KL. 2019. Six-week high-fat diet alters the gut microbiome and promotes cecal inflammation, endotoxin production, and simple steatosis without obesity in male rats. *Lipids* **54(2–3)**:119–131 DOI 10.1002/lipd.12131.

Cuspidi C, Sala C, Provenzano F, Tadic M, Gherbesi E, Grassi G, Mancia G. 2018. Metabolic syndrome and subclinical carotid damage: a meta-analysis from population-based studies. *Journal of Hypertension* **36(1)**:23–30 DOI 10.1097/HJH.0000000000001575.

Dahm CC, Chomistek AK, Jakobsen MU, Mukamal KJ, Eliassen AH, Sesso HD, Overvad K, Willett WC, Rimm EB, Chiuve SE. 2016. Adolescent diet quality and cardiovascular disease risk factors and incident cardiovascular disease in middle-aged women. *Journal of the American Heart Association* **5(12)**:96 DOI 10.1161/JAHA.116.003583.

Daugaard M, Rohde M, Jäättelä M. 2007. The heat shock protein 70 family: highly homologous proteins with overlapping and distinct functions. *FEBS Letters* **581(19)**:3702–3710 DOI 10.1016/j.febslet.2007.05.039.

Dulin E, García-Barreno P, Guisasola MC. 2012. Genetic variations of HSPA1A, the heat shock protein levels, and risk of atherosclerosis. *Cell Stress and Chaperones* **17(4)**:507–516 DOI 10.1007/s12192-012-0328-4.

Fedorova O, Petukhov A, Daks A, Shuvalov O, Leonova T, Vasileva E, Aksenov N, Melino G, Barlev NA. 2019. Orphan receptor NR4A3 is a novel target of p53 that contributes to apoptosis. *Oncogene* **38(12)**:2108–2122 DOI 10.1038/s41388-018-0566-8.

Fortuño A, Rodríguez A, Gómez-Ambrosi J, Muñiz P, Salvador J, Díez J, Frühbeck G. 2002. Leptin inhibits angiotensin II-induced intracellular calcium increase and vasoconstriction in the rat aorta. *Endocrinology* **143(9)**:3555–3560 DOI 10.1210/en.2002-220075.

Franssens BT, Hoogduin H, Leiner T, Van der Graaf Y, Visseren FLJ. 2017. Relation between brown adipose tissue and measures of obesity and metabolic dysfunction in patients with cardiovascular disease. *Journal of Magnetic Resonance Imaging* **46(2)**:497–504 DOI 10.1002/jmri.25594.

Fridlyand LE, Philipson LH. 2006. Reactive species and early manifestation of insulin resistance in type 2 diabetes. *Diabetes, Obesity & Metabolism* **8(2)**:136–145 DOI 10.1111/j.1463-1326.2005.00496.x.

Friederich-Persson M, Nguyen Dinh Cat A, Persson P, Montezano AC, Touyz RM. 2017. Brown adipose tissue regulates small artery function through NADPH oxidase 4-derived hydrogen

peroxide and redox-sensitive protein kinase G-1. *Arteriosclerosis, Thrombosis, and Vascular Biology* **37(3)**:455–465 DOI 10.1161/ATVBAHA.116.308659.

Gimbrone MA Jr, García-Cardeña G. 2016. Endothelial cell dysfunction and the pathobiology of atherosclerosis. *Circulation Research* **118(4)**:620–636 DOI 10.1161/CIRCRESAHA.115.306301.

Han S, Cohen DE. 2012. Functional characterization of thioesterase superfamily member 1/Acyl-CoA thioesterase 11: implications for metabolic regulation. *Journal of Lipid Research* **53(12)**:2620–2631 DOI 10.1194/jlr.M029538.

Hess K, Oliverio R, Nguyen P, Le D, Ellis J, Kdeiss B, Ord S, Chalkia D, Nikolaidis N. 2018. Concurrent action of purifying selection and gene conversion results in extreme conservation of the major stress-inducible Hsp70 genes in mammals. *Scientific Reports* **8(1)**:5082 DOI 10.1038/s41598-018-23508-x.

Hildebrand S, Stümer J, Pfeifer A. 2018. PVAT and its relation to brown, beige, and white adipose tissue in development and function. *Frontiers in Physiology* **9**:70 DOI 10.3389/fphys.2018.00070.

Hintze KJ, Benninghoff AD, Cho CE, Ward RE. 2018. Modeling the western diet for preclinical investigations. *Advances in Nutrition* **9(3)**:263–271 DOI 10.1093/advances/nmy002.

Hurrle S, Hsu WH. 2017. The etiology of oxidative stress in insulin resistance. *Biomedical Journal* **40(5)**:257–262 DOI 10.1016/j.bj.2017.06.007.

Hutter MM, Sievers RE, Barbosa V, Wolfe CL. 1994. Heat-shock protein induction in rat hearts: a direct correlation between the amount of heat-shock protein induced and the degree of myocardial protection. *Circulation* **89(1)**:355–360 DOI 10.1161/01.CIR.89.1.355.

Jiang HK, Qiu GR, Li-Ling J, Xin N, Sun KL. 2010. Reduced ACTC1 expression might play a role in the onset of congenital heart disease by inducing cardiomyocyte apoptosis. *Circulation Journal* **74(11)**:2410–2418 DOI 10.1253/circj.CJ-10-0234.

Kassi E, Pervanidou P, Kaltsas G, Chrousos G. 2011. Metabolic syndrome: definitions and controversies. *BMC Medicine* **9(1)**:48 DOI 10.1186/1741-7015-9-48.

Katsiki N, Athyros VG, Karagiannis A, Mikhailidis DP. 2014. Metabolic syndrome and non-cardiac vascular diseases: an update from human studies. *Current Pharmaceutical Design* **20(31)**:4944–4952 DOI 10.2174/1381612819666131206100750.

Kvam VM, Liu P, Si Y. 2012. A comparison of statistical methods for detecting differentially expressed genes from RNA-seq data. *American Journal of Botany* **99(2)**:248–256 DOI 10.3732/ajb.1100340.

Li X, Cooper NGF, O'Toole TE, Rouchka EC. 2020. Choice of library size normalization and statistical methods for differential gene expression analysis in balanced two-group comparisons for RNA-seq studies. *BMC Genomics* **21(1)**:75 DOI 10.1186/s12864-020-6502-7.

Marioni JC, Mason CE, Mane SM, Stephens M, Gilad Y. 2008. RNA-seq: an assessment of technical reproducibility and comparison with gene expression arrays. *Genome Research* **18(9)**:1509–1517 DOI 10.1101/gr.079558.108.

Maza E. 2016. In Papyro comparison of TMM (edgeR), RLE (DESeq2), and MRN normalization methods for a simple two-conditions-without-replicates RNA-Seq experimental design. *Frontiers in Genetics* **7**:164 DOI 10.3389/fgene.2016.00164.

McCallister C, Siracusa MC, Shirazi F, Chalkia D, Nikolaidis N. 2015. Functional diversification and specialization of cytosolic 70-kDa heat shock proteins. *Scientific Reports* **5(1)**:9363 DOI 10.1038/srep09363.

Mendoza J, Pévet P, Challet E. 2008. High-fat feeding alters the clock synchronization to light. *Journal of Physiology* **586(24)**:5901–5910 DOI 10.1113/jphysiol.2008.159566.

Mia S, Sonkar R, Williams L, Latimer MN, Frayne Robillard I, Diwan A, Frank SJ, Des Rosiers C, Young ME. 2021. Impact of obesity on day-night differences in cardiac metabolism. *FASEB Journal* **35(3)**:e21298 DOI 10.1096/fj.202001706RR.

Milenkovic D, Paslawski R, Gomulkiewicz A, Gladine C, Janczak D, Grzegorek I, Jablonska K, Drozdz K, Chmielewska M, Piotrowska A, Janiszewski A, Dziegiel P, Mazur A, Paslawska U, Szuba A. 2020. Alterations of aorta intima and media transcriptome in swine fed high-fat diet over 1-year follow-up period and of the switch to normal diet. *Nutrition, Metabolism and Cardiovascular Diseases* **30(7)**:1201–1215 DOI 10.1016/j.numecd.2020.04.007.

Moore JX, Chaudhary N, Akinyemiju T. 2017. Metabolic syndrome prevalence by race/ethnicity and sex in the United States, National Health and Nutrition examination survey, 1988–2012. *Preventing Chronic Disease* **14**:160287 DOI 10.5888/pcd14.160287.

Nernpermpisooth N, Qiu S, Mintz JD, Suvitayavat W, Thirawarapan S, Rudic DR, Fulton DJ, Stepp DW. 2015. Obesity alters the peripheral circadian clock in the aorta and microcirculation. *Microcirculation* **22(4)**:257–266 DOI 10.1111/micc.12192.

Ning H, Labarthe DR, Shay CM, Daniels SR, Hou L, Van Horn L, Lloyd-Jones DM. 2015. Status of cardiovascular health in US children up to 11 years of age. *Circulation: Cardiovascular Quality and Outcomes* **8(2)**:164–171 DOI 10.1161/CIRCOUTCOMES.114.001274.

Oda A, Taniguchi T, Yokoyama M. 2001. Leptin stimulates rat aortic smooth muscle cell proliferation and migration. *Kobe Journal of Medical Sciences* **47(3)**:141–150.

Oita RC, Mazzatti DJ, Lim FL, Powell JR, Merry BJ. 2009. Whole-genome microarray analysis identifies up-regulation of Nr4a nuclear receptors in muscle and liver from diet-restricted rats. *Mechanisms of Ageing and Development* **130(4)**:240–247 DOI 10.1016/j.mad.2008.12.004.

Okada K, LeClair KB, Zhang Y, Li Y, Ozdemir C, Krisko TI, Hagen SJ, Betensky RA, Banks AS, Cohen DE. 2016. Thioesterase superfamily member 1 suppresses cold thermogenesis by limiting the oxidation of lipid droplet-derived fatty acids in brown adipose tissue. *Molecular Metabolism* **5(5)**:340–351 DOI 10.1016/j.molmet.2016.02.002.

Omotola O, Legan S, Slade E, Adekunle A, Pendergast JS. 2019. Estradiol regulates daily rhythms underlying diet-induced obesity in female mice. *American Journal of Physiology-Endocrinology and Metabolism* **317(6)**:E1172–E1181 DOI 10.1152/ajpendo.00365.2019.

Osawa H, Printz RL, Whitesell RR, Granner DK. 1995. Regulation of hexokinase II gene transcription and glucose phosphorylation by catecholamines, cyclic AMP, and insulin. *Diabetes* **44(12)**:1426–1432 DOI 10.2337/diab.44.12.1426.

Palmisano BT, Stafford JM, Pendergast JS. 2017. High-fat feeding does not disrupt daily rhythms in female mice because of protection by ovarian hormones. *Perspectives on Assisted Reproduction* **8**:44 DOI 10.3389/fendo.2017.00044.

Pan H, Guo J, Su Z. 2014. Advances in understanding the interrelations between leptin resistance and obesity. *Physiology & Behavior* **130(5)**:157–169 DOI 10.1016/j.physbeh.2014.04.003.

Pearen MA, Eriksson NA, Fitzsimmons RL, Goode JM, Martel N, Andrikopoulos S, Muscat GEO. 2012. The nuclear receptor, Nor-1, markedly increases type II oxidative muscle fibers and resistance to fatigue. *Molecular Endocrinology* **26(3)**:372–384 DOI 10.1210/me.2011-1274.

Petrie JR, Guzik TJ, Touyz RM. 2018. Diabetes, hypertension, and cardiovascular disease: clinical insights and vascular mechanisms. *Canadian Journal of Cardiology* **34(5)**:575–584 DOI 10.1016/j.cjca.2017.12.005.

Prosser RA, Bergeron HE. 2003. Leptin phase-advances the rat suprachiasmatic circadian clock in vitro. *Neuroscience Letters* **336(3)**:139–142 DOI 10.1016/S0304-3940(02)01234-X.

Quindry JC, Hamilton KL, French JP, Lee Y, Murlasits Z, Tumer N, Powers SK. 2007. Exercise-induced HSP-72 elevation and cardioprotection against infarct and apoptosis. *Journal of Applied Physiology* **103(3)**:1056–1062 DOI 10.1152/japplphysiol.00263.2007.

Radford NB, Fina M, Benjamin IJ, Moreadith RW, Graves KH, Zhao P, Gavva S, Wiethoff A, Sherry AD, Malloy CR, Williams RS. 1996. Cardioprotective effects of 70-kDa heat shock protein in transgenic mice. *Proceedings of the National Academy of Sciences of the United States of America* **93(6)**:2339–2342 DOI 10.1073/pnas.93.6.2339.

Ramsey KM, Yoshino J, Brace CS, Abrassart D, Kobayashi Y, Marcheva B, Hong HK, Chong JL, Buhr ED, Lee C, Takahashi JS, Imai S, Bass J. 2009. Circadian clock feedback cycle through NAMPT-mediated NAD+ biosynthesis. *Science* **324(5927)**:651–654 DOI 10.1126/science.1171641.

Rao MS, Van Vleet TR, Ciurlionis R, Buck WR, Mittelstadt SW, Blomme EAG, Liguori MJ. 2019. Comparison of RNA-Seq and microarray gene expression platforms for the toxicogenomic evaluation of liver from short-term rat toxicity studies. *Frontiers in Genetics* **9**:636 DOI 10.3389/fgene.2018.00636.

Reddy SS, Shruthi K, Prabhakar YK, Sailaja G, Reddy GB. 2018. Implication of altered ubiquitin-proteasome system and ER stress in the muscle atrophy of diabetic rats. *Archives of Biochemistry and Biophysics* **639(5)**:16–25 DOI 10.1016/j.abb.2017.12.015.

Reiss RA, Guerra P, Makhnin O. 2016. Metagenome phylogenetic profiling of microbial community evolution in a tetrachloroethene-contaminated aquifer responding to enhanced reductive dechlorination protocols. *Standards in Genomic Sciences* **11(1)**:88 DOI 10.1186/s40793-016-0209-z.

Reiss RA, Lowe TC, Sena JA, Makhnin O, Connick MC, Illescas PE, Davis CF. 2020. Bio-activating ultrafine grain titanium: RNA sequencing reveals enhanced mechano-activation of osteoconduction on nanostructured substrates. *PLOS ONE* **15(9)**:e0237463 DOI 10.1371/journal.pone.0237463.

Richter K, Haslbeck M, Buchner J. 2010. The heat shock response: life on the verge of death. *Molecular Cell* **40(2)**:253–266 DOI 10.1016/j.molcel.2010.10.006.

Robinson MD, McCarthy DJ, Smyth GK. 2010. EdgeR: a bioconductor package for differential expression analysis of digital gene expression data. *Bioinformatics* **26(1)**:139–140 DOI 10.1093/bioinformatics/btp616.

Rodríguez-Correa E, González-Pérez I, Clavel-Pérez PI, Contreras-Vargas Y, Carvajal K. 2020. Biochemical and nutritional overview of diet-induced metabolic syndrome models in rats: what is the best choice? *Nutrition & Diabetes* **10(1)**:24 DOI 10.1038/s41387-020-0127-4.

Saltiel AR, Kahn CR. 2001. Insulin signalling and the regulation of glucose and lipid metabolism. *Nature* **414(6865)**:799–806 DOI 10.1038/414799a.

Shin HJ, Oh J, Kang SM, Lee JH, Shin MJ, Hwang KC, Jang Y, Chung JH. 2005. Leptin induces hypertrophy via p38 mitogen-activated protein kinase in rat vascular smooth muscle cells. *Biochemical and Biophysical Research Communications* **329(1)**:18–24 DOI 10.1016/j.bbrc.2004.12.195.

Silverman ES, Collins T. 1999. Pathways of Egr-1-mediated gene transcription in vascular biology. *American Journal of Pathology* **154(3)**:665–670 DOI 10.1016/S0002-9440(10)65312-6.

Su W, Xie Z, Guo Z, Duncan MJ, Lutshumba J, Gong MC. 2012. Altered clock gene expression and vascular smooth muscle diurnal contractile variations in type 2 diabetic db/db mice. *American Journal of Physiology. Heart and Circulatory Physiology* **302(3)**:H621–H633 DOI 10.1152/ajpheart.00825.2011.

Sundaram S, Johnson LK, Yan L. 2020. High-fat diet alters circadian rhythms in mammary glands of pubertal mice. *Perspectives on Assisted Reproduction* **11**:349 DOI 10.3389/fendo.2020.00349.

Sweazea KL, Lekic M, Walker BR. 2010. Comparison of mechanisms involved in impaired vascular reactivity between high sucrose and high fat diets in rats. *Nutrition & Metabolism* **7(1)**:48 DOI 10.1186/1743-7075-7-48.

Sweazea KL, Walker BR. 2011. High fat feeding impairs endothelin-1 mediated vasoconstriction through increased iNOS-derived nitric oxide. *Hormone and Metabolic Research* **43(7)**:470–476 DOI 10.1055/s-0031-1273763.

Sweazea KL, Walker BR. 2012. Impaired myogenic tone in mesenteric arteries from overweight rats. *Nutrition & Metabolism* **9(1)**:18 DOI 10.1186/1743-7075-9-18.

Tao W, Wu J, Zhang Q, Lai SS, Jiang S, Jiang C, Xu Y, Xue B, Du J, Li CJ. 2015. EGR1 regulates hepatic clock gene amplitude by activating Per1 transcription. *Scientific Reports* **5(1)**:15212 DOI 10.1038/srep15212.

Trapnell C, Pachter L, Salzberg SL. 2009. TopHat: discovering splice junctions with RNA-Seq. *Bioinformatics* **25(9)**:1105–1111 DOI 10.1093/bioinformatics/btp120.

Triggle CR, Samuel SM, Ravishankar S, Marei I, Arunachalam G, Ding H. 2012. The endothelium: influencing vascular smooth muscle in many ways. *Canadian Journal of Physiology and Pharmacology* **90(6)**:713–738 DOI 10.1139/y2012-073.

Xu J, Yang G, Li T, Liu L. 2017. Myoendothelial gap junctions mediate regulation of angiopoietin-2-induced vascular hyporeactivity after hypoxia through connexin 43-gated cAMP transfer. *American Journal of Physiology-Cell Physiology* **313(3)**:C262–C273 DOI 10.1152/ajpcell.00369.2016.

Wang CY, Liu HJ, Chen HJ, Lin YC, Wang HH, Hung TC, Yeh HI. 2011. AGE-BSA down-regulates endothelial connexin43 gap junctions. *BMC Cell Biology* **12(1)**:19 DOI 10.1186/1471-2121-12-19.

Wang P, Miao CY. 2015. NAMPT as a therapeutic target against stroke. *Trends in Pharmacological Sciences* **36(12)**:891–905 DOI 10.1016/j.tips.2015.08.012.

Wiernsperger NF. 2003. Oxidative stress as a therapeutic target in diabetes: revisiting the controversy. *Diabetes & Metabolism* **29(6)**:579–585 DOI 10.1016/S1262-3636(07)70072-1.

Wong RH, Sul HS. 2010. Insulin signaling in fatty acid and fat synthesis: a transcriptional perspective. *Current Opinion in Pharmacology* **10(6)**:684–691 DOI 10.1016/j.coph.2010.08.004.

Wu TD, Watanabe CK. 2005. GMAP: a genomic mapping and alignment program for mRNA and EST sequences. *Bioinformatics* **21(9)**:1859–1875 DOI 10.1093/bioinformatics/bti310.

Xi D, Zhao J, Zhao M, Fu W, Guo Z, Chen H. 2017. Identification of gene expression changes in the aorta of ApoE null mice fed a high-fat diet. *Genes* **8(10)**:289 DOI 10.3390/genes8100289.

Yan SF, Fujita T, Lu J, Okada K, Shan Zou Y, Mackman N, Pinsky DJ, Stern DM. 2000. Egr-1, a master switch coordinating upregulation of divergent gene families underlying ischemic stress. *Nature Medicine* **6(12)**:1355–1361 DOI 10.1038/82168.

Yin L, Wu N, Curtin JC, Qatanani M, Szwergold NR, Reid RA, Waitt GM, Parks DJ, Pearce KH, Wisely GB, Lazar MA. 2007. Rev-erbalpha, a heme sensor that coordinates metabolic and circadian pathways. *Science* **318(5857)**:1786–1789 DOI 10.1126/science.1150179.

Zhang Y, Li Y, Niepel MW, Kawano Y, Han S, Liu S, Marsili A, Larsen PR, Lee CH, Cohen DE. 2012. Targeted deletion of thioesterase superfamily member 1 promotes energy expenditure and protects against obesity and insulin resistance. *Proceedings of the National Academy of Sciences of the United States of America* **109(14)**:5417–5422 DOI 10.1073/pnas.1116011109.